Korean J. of Chem. Eng., **6**(3) (1989) *212-218*

MASS TRANSFER BETWEEN AN EDDY OF CAVITY AND ADJACENT FLOWS

Joong Kon PARK*, Hwa Won RYU, and Ho Nam CHANG**

*Department of Chemical Engineering, Kyungpook National University, Taegu 702-701, Korea
Department of Chemical Engineering, Chonnam National University, Kwang-ju 500-757, Korea
**Department of Chemical Engineering, Korea Advanced Institute of Science and Technology, P.O. Box 131 Cheongryang, Seoul, Korea

(Received 8 September 1988 • accepted 18 January 1989)

Abstract—Mass Transfer from a cavity containing an eddy to the main contacting flow was investigated by computer simulation and visualization experiments. The mass transfer between the cavity and the main contacting flow was affected mainly by the rotation of the eddy and correlated as $Sh = 2.29 \times 10^{-5} Re^{2.18} Sc^{1.03} AR^{0.156}$ where AR is the aspect ratio ranging from 1 to 4. The Reynolds number was varied from 25 to 100 and the Schmidt number from 100 to 10000.

INTRODUCTION

In chemical and biological reactors existence of stagnant region is not uncommon, where no convectional mixing with the main flow takes place. Park and Chang [1] showed numerically that an eddy can form in the front head of a hollow fiber artificial kidney. Blood within the eddy formed in the artificial kidney stays longer in the device than the mean residence time of the system, which results in blood coagulation leading to the occlusion of the fibers and lower efficiency of the dialyzer. In a packed bed reactor a stagnant region can form in the rear of a spherical packing. The presence of stagnant regions in any kind of reactors usually results in lower mass transfer and reactor efficiency. The mass transfer between stagnant regions and the main flow has not been studied much in contrast to numerous studies of fluid mechanics in the cavities.

In order to understand the mass transfer between the stagnant region and the main contacting flow, it is necessary to investigate systematically the mass transfer from a well-defined stagnant region. The rectangular cavity connected to the main contacting flow shown in Fig. 1 was chosen as a model of the system because the fluid in the cavity is not mixed with the main flow and an eddy is easily formed. Charwat et al. [2] proposed the mass exchanged model to explain the process of heat transfer in a shallow cavity at supersonic or subsonic flow region. But this model does not seem adequate for deeper cavities. Haugen and Dhanak [3] studied heat transfer in turbulent flow with conditions of uniform temperature and uniform heat flux at cavity walls. Kang and Chang [4] numerically investigated the hydrodynamic performance of cavity type and zigzag type turbulence promoters and proposed an empirical correlation for Sherwood number in terms of both Reynolds number and Schmidt number. Kim et al. [5] measured local mass transfer rates on the wall with the limiting current method and compared their results with those obtained by Kang and Chang [4], Weiss and Florsheim [6] investigated the flow in cavities with high AR under the condition of creeping flow. Prata and Sparrow [7,8] measured the evaporation rate of volatile liquid from an open-topped container to an air stream. But the mass transfer from the cavity to the main flow in a single phase was not studies. Thus the rate of mass transfer at the interface between the mass flow and the cavity whose wall was inert was calculated by numerical analysis of the governing momentum and mass balance equations. The flow visualization experiment was performed in order to verify the numerical predictions indirectly. The numerical results of mass transfer were expressed in terms of Sherwood number as a function of the Reynolds number, the Schmidt number and the aspect ratio of the cavity.

** To whom all correspondence should be addressed.

COMPUTATIONAL ANALYSIS

Dimensionless governing equations for the vorticity, the stream function and the mass in rectangular co-

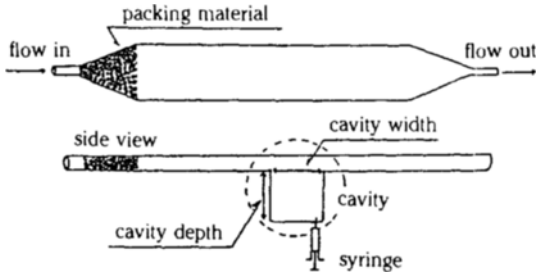

Fig. 1. Schematic diagram of the system for eddy mass transfer study.

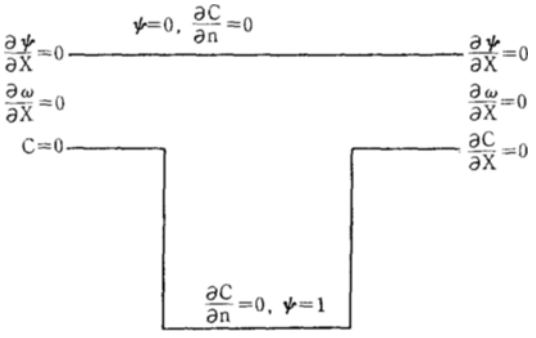

Fig. 2. Boundary conditions.

ordinate can be written as follows:

$$u\frac{\partial \omega}{\partial x}+v\frac{\partial \omega}{\partial y}=\frac{1}{Re}\left(\frac{\partial^2 \omega}{\partial x^2}+\frac{\partial^2 \omega}{\partial y^2}\right) \quad (1)$$

$$\omega=\frac{\partial^2 \psi}{\partial x^2}+\frac{\partial^2 \psi}{\partial y^2} \quad (2)$$

$$\frac{\partial C}{\partial t}=-u\frac{\partial C}{\partial x}-v\frac{\partial C}{\partial y}+\frac{1}{Pe}\left(\frac{\partial^2 C}{\partial x^2}+\frac{\partial^2 C}{\partial y^2}\right) \quad (3)$$

$C=1$ at $t=0$

$C=0$ at $x=0$

$\frac{\partial C}{\partial n}=0$ at wall of the system

where the Reynolds number Re is based on the height of the main channel H and the average velocity in the main channel U_o. The characteristic length is the height of the channel and the dimensionless time is defined as $t = U_oT/H$.

The governing equations are solved by the finite difference method. The vorticity transport equation is discretized according to the first upwind difference form and variable grid space is introduced to the system. Grid lines are concentrated in the region where the fluid motion varied abruptly. Near the wall the ratio does not exceed 1.5 at any point as suggested by Gosman et al. [9]. The Gauss-Seidel method is used to solve the stream function equation and the under-relaxation method is used for the vorticity transport equation. The initial values of the stream function and the vorticity are assumed at all grid points. Then with the boundary conditions given in Fig. 2 the computation is continued until the stream function and vorticity converge. The convergence condition is such that the relative error

$$E=\frac{|\psi_{ij}^{n}-\psi_{ij}^{n-1}|}{|\psi_{max}^{n-1}|}$$

is less than 1.0×10^{-4} at all grid points. With the calculated results of fluid motion, the concentration distribution in the cavity at any time is calculated by the parabolic unsteady-state mass transfer equation. The initial values of the dimensionless concentration are 1 at all grid points. The increment of dimensionless time was less than 0.05 for the stability of the numerical scheme. Upstream of the main channel, Dirichlet boundary conditions are used for the stream function and the vorticity, and the concentration is zero because pure water comes in. These seem appropriate when there is no information available for the fluid velocity in that region. At the solid wall vorticity is of the first order form as

$$\omega=\frac{2(\psi_{wall+1}-\psi_{wall})}{\Delta n^2} \quad (4)$$

and the concentration derivative is zero because there is no mass transfer at the wall surface. Downstream of the main channel, Dirichlet boundary conditions are used for the stream function, the vorticity and the concentration.

COMPUTATIONAL RESULTS

The computed streamline distribution and the transient contour maps of the concentration in the cavity for AR = 1 and Re = 100 are shown in Fig. 3 where AR is the aspect ratio of the cavity defined as the cavity depth divided by the cavity width. A large eddy is formed in the cavity and the center of circulation of this eddy leans slightly toward right upper region. The initial concentration in the cavity and the main channel are C_o. From time T=0 the fresh solution comes from the inlet of the main channel. The mean concentrations in the cavity are $0.94C_o$, $0.84C_o$, and $0.03C_o$ after 18, 72, 3502 seconds, respectively. The material is transferred from the cavity to the main channel at the interface, and the fluid in the cavity is mixed by the circulation of the eddy. The refreshed solution penetrates into the cavity from the upper right corner because the vortex rotates in a clockwise direc-

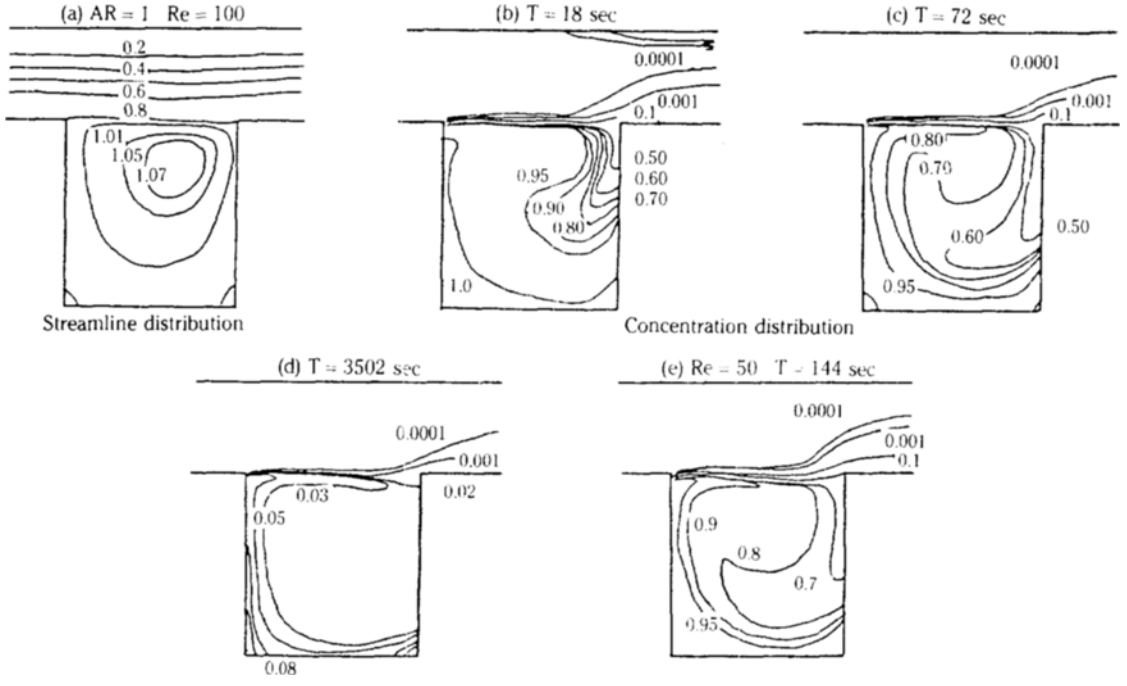

Fig. 3. Streamline and concentration distribution in the cavity system (Sc = 1000).
(a) streamline distribution for AR = 1, Re = 100
(b, c, d) concentration distribution for AR = 1, Re = 100
(e) concentration distribution for AR = 1, Re = 50

tion. As time elapses, the concentration in the cavity is diluted first at the right side and then the diluted concentration contours move progressively in a clockwise direction. After sufficient time (T = 3502 seconds) has elapsed, the concentration at the major portion of the cavity falls below $0.05C_o$, and the maximum concentration is found at the lower left and right corners of the cavity where the weak secondary eddies are located. It is expected that the tracer at the lower left corner is depleted last. The concentration distribution in the cavity after 144 seconds for AR = 1, Re = 50 and Sc = 1000 is shown in Fig. 3(e). The mechanism of mixing of the material in the cavity is similar to the case for Re = 100, but the concentration at the right upper region for T = 144 seconds is slightly higher than that for Re = 100. This is believed to occur due to the weaker rotation of the eddy in the cavity. When AR is increased to 3, two more vortices appear at the lower part of the cavity [Fig. 4(a)]. The rotating velocities of the second and third eddy are about 10^{-3} and 10^{-6} times that of the first. Figure 4 shows that at an earlier stage (T = 72 seconds) the contour lines of the concentration are very similar to those of AR = 1, but the depletion region is limited to the first eddy. As time passes, the concentration contour lines move into the cavity at the left side due to the reverse direction of the rotation of the secondary vortex. Below the region where the secondary vortex is located, diffusional mass transfer occurs after a sufficient lapse of time. After 1000 seconds the concentration in the first eddy is less than $0.2C_o$, but that in the second eddy is still higher than $0.9C_o$ and in the third eddy is about $1.0C_o$. Chang et al. [10] concluded that in the cavity containing three or more eddies convectional mass transfer due to rotation of eddy was limited in the first eddy and convectional mass transfer from one side of the cavity to the other side was largely greater than that by the diffusion. Thus it is natural to recognize that the rotation speed of vortex plays an important role in this study. In Fig. 5 the contour maps of the concentration and the stream function are plotted together. In the case of AR = 1 and T = 42 seconds the protruded concentration lines lie on the streamlines, showing that the convective flow introduces the fresh solution into the cavity. In order to confirm this computational results the movement of the tracer in the cavity was photographed (Fig. 6). The black ink tracer was introduced by pulse into the cavity of AR = 1 with the syringe (Fig. 1). As predicted in the computer simulation, we can see that the fresh solution penetrates into the cavity

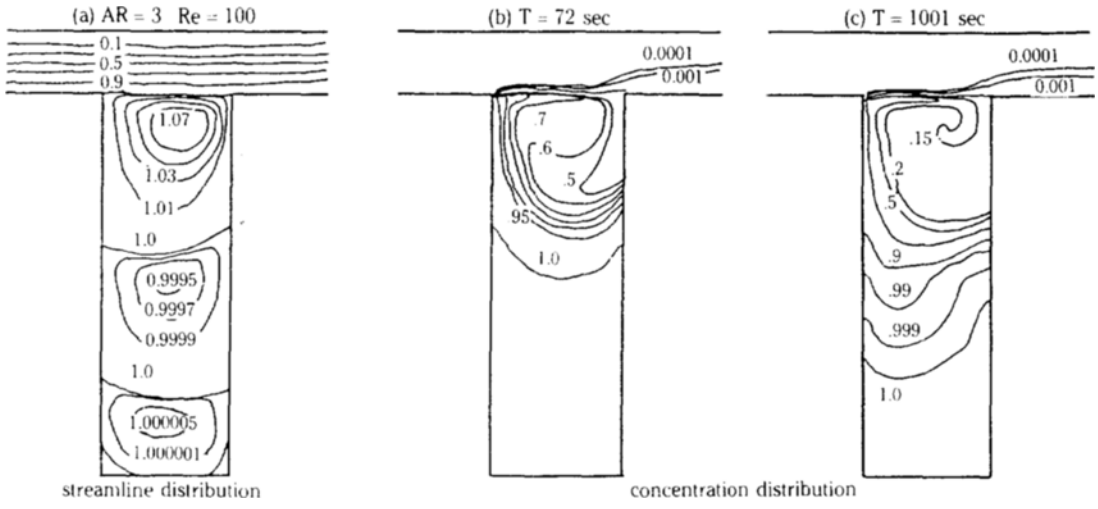

Fig. 4. Streamline and concentration distributions in deep cavity system (Sc = 1000, Re = 100).

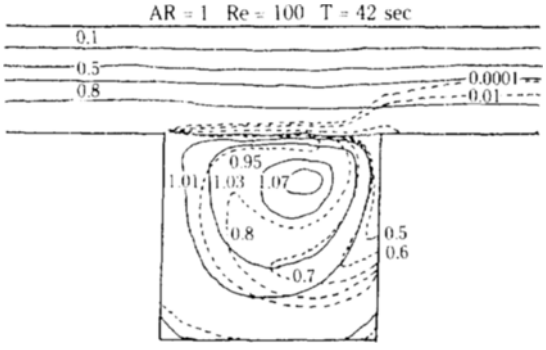

Fig. 5. Overlapping contour maps of the concentration and stream function.

from the upper right corner of the cavity and flows in a clockwise direction as the vortex rotates. As time passes, the concentration of the dye becomes lower progressively and in the middle region of the cavity the concentration is lower than that in the surrounding region. This confirms that the main driving force of the mixing and transfer of the material is attributed to the rotation of the eddy.

MASS TRANSFER FROM THE CAVITY

From the computational results and the photographs of the tracer motion it can be concluded that the material in the cavity is mixed by the rotation of the eddy and transferred from the cavity to the main channel through the boundary surface between the channel and the cavity. The overall mass transfer from the cavity can be described as follows:

$$N = k(C_b - C_s)$$

From the balance in the cavity.

$$V\frac{dC_b}{dt} = -NA \tag{6}$$

where V is the volume of the cavity, and A is the boundary surface area between the cavity and the main channel, C_b refers to the mean concentration of the material in the cavity and is calculated from the computational results C_s is the concentration at the boundary surface. From the computational results C_s is about 10^{-3} C_o and can be neglected as compared with C_b. Then equations 5 and 6 can be simplified as

$$H\frac{dC_b}{dt} = -kC_b \tag{7}$$

where H is the depth of the cavity. Integration of equation 7 gives

$$\ln\frac{C_o}{C_b} = \frac{k}{H}t \tag{8}$$

The mass transfer coefficient k divided by H is the slope of the concentration if the logarithmic concentration is plotted against time. The plot of concentration with time is shown in Fig. 7, from which the mass transfer coefficient k is 6.98×10^{-3} cm/sec for Re = 100, AR = 1 and Sc = 1000. The mass transfer coefficients for each conditions are tabulated in Table 1. The mass transfer coefficient becomes higher with the increase of the Reynolds number and its dependence on the Schmidt number is very small. When the Schmidt number is varied in the range of 500 to 10000 in the computational calculation for AR = 1, the contour lines remain unchanged. Thus it can be concluded that the

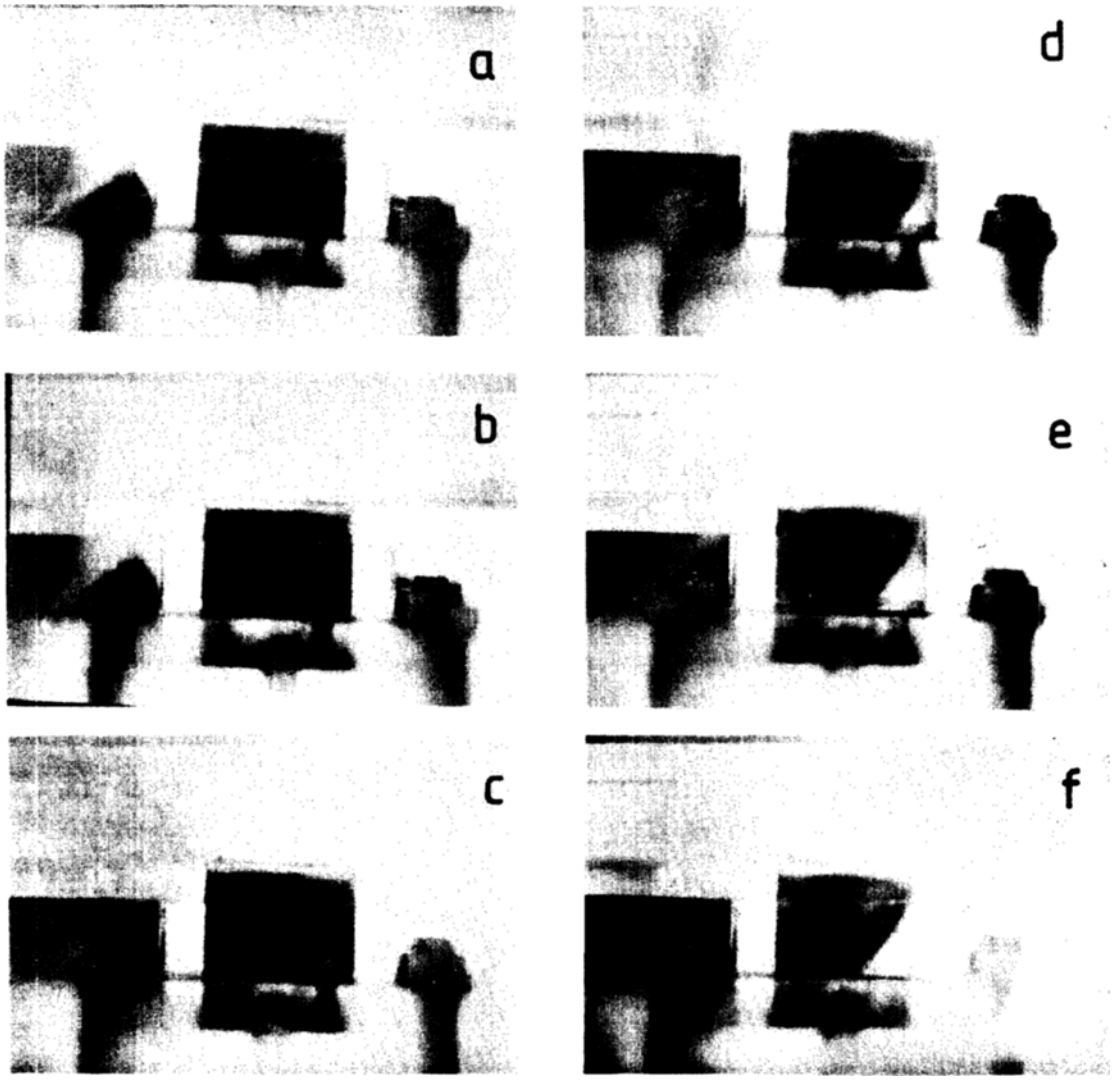

Fig. 6. Photographs for the movement of dye (AR = 1, Re = 100).
After (a) 15sec (b) 120sec (c) 360sec (d) 480sec (e) 600sec (f) 720sec from the injection of dye.

effect of the rotational speed of the eddy on the mass transfer for this system is more important than the diffusional effect. In other words, the convectional transport is much faster than the diffusional transport. This can be also seen in two phase system. Prata and Sparrow [8] showed experimentally that the Sherwood number and the Schmidt number were linearly related when volatile liquids evaporated from an open-topped, partially filled container to an air system. The mass transfer coefficient for AR = 1 is smaller than that for any other higher value of AR. And those of AR = 2, 3 and 4 are nearly the same value with little deviations. This can be explained by the eddy formation and mechanism of the mixing of the material in the cavity. In the cavities with AR value larger than 1 the main region of mixing and mass transfer is limited to the first eddy, but the size of this first eddy is little larger than that of AR = 1. The total quantity which has been removed from the cavity to the main flow after 120 seconds from the initial point of operation is shown in Table 2. The quantity of the material removed from the cavity of AR = 1 is 25% smaller than those of AR = 2, 3, 4 that are the same. The result supports the above explanation regarding the variation of mass transfer coefficient with AR. Figure 8 shows that the mass transfer rate from the cavity with an eddy to the

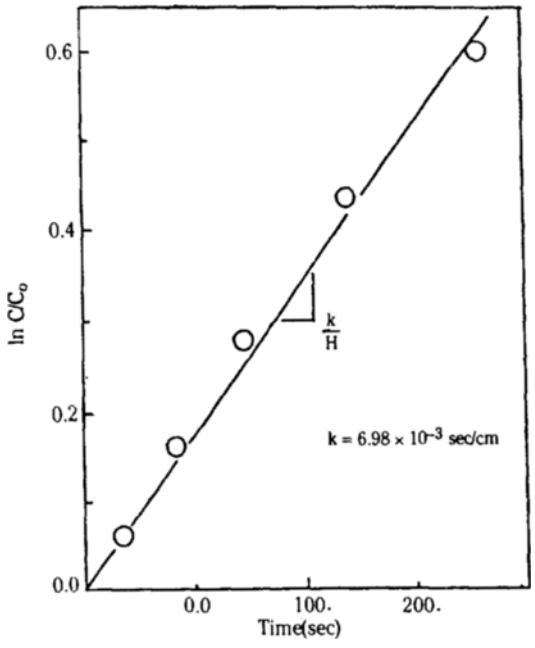

Fig. 7. Mean concentration in the cavity with time (AR = 1, Re = 100, Sc = 1000).

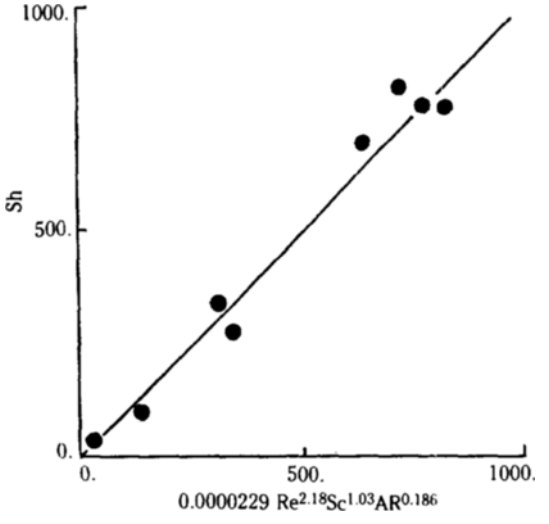

Fig. 8. Correlation of Sherwood number as a function of Re, Sc, and AR.

channel is correlated as $Sh = 2.29 \times 10^{-5} Re^{2.18} Sc^{1.03} AR^{0.186}$.

CONCLUSION

For a cavity system in which an eddy can be formed by the shear motion of the contacting main flow, the material trapped in the cavity does not easily move out to the main flow channel. The material in the cavity is mixed by the rotation of an eddy and the main driving force for the mass transfer from the cavity to the main channel is not the diffusivity of the matter but the rotational speed of an eddy. The mass transfer rate from the cavity to the main channel is quantified as

$$Sh = 2.29 \times 10^{-5} Re^{2.18} Sc^{1.03} AR^{0.186}$$

ACKNOWLEDGEMENT

The authors are indebted to the Korea Science and Engineering Foundation (KOSEF) for partial support of this research.

NOMENCLATURE

AR : aspect ratio of the cavity, dimensionless value of the depth of the cavity divided by the cavity width
C : dimensionless concentration, concentration/C_o
C_o : initial concentration in the cavity, mol/m^3
C_b : mean concentration in the cavity, mol/m^3
D : diffusion coefficient, m/sec
H : depth of the cavity, m
k : mass transfer coefficient, m/sec
L : height of the main channel, m
N : mass flux, mol/m^2/sec
Pe : Peclet number, D/U_oL
Re : Reynolds number, U_oL/ν
Sc : Schmidt number, ν/D
Sh : Sherwood number, kL/D
T : time, sec
t : dimensionless time, U_oT/L
U_o : mean fluid velocity in the channel, m/sec
u : fluid velocity in the x direction, m/sec
v : fluid velocity in the y direction, m/sec
x : x coordinate
y : y coordinate

Greek Letters

ν : kinematic viscosity
ρ : density
ψ : stream function
ω : vorticity

Subscripts

c : cavity
c_1 : cavity with AR = 1

REFERENCES

1. Park, J.K. and Chang, H.N.: *AIChE J.*, **32,** 1937 (1986).
2. Charwat, A.F., Roos, J.N., Dewey, F.C. Jr., and Hitz, J.A.: *J. Aerospace Sci.*, **28,** 457 (1961).
3. Haugen, R.L. and Dhanak, A.M.: *J. Heat Trans., Trans. ASME,* **89,** 335 (1967).
4. Kang, I.S. and Chang, H.N.: *Int'l. J. Heat & Mass Transfer,* **25,** 1167 (1982).
5. Kim, D.H., Kim, I.H., and Chang, H.N.: *Int'l. J. Heat & Mass Transfer,* **26,** 1007 (1983).
6. Weiss, R.F. and Florsheim, B.H.: *Physics of Fluids,* **8,** 1631 (1965).
7. Prata, A.T. and Sparrow, E.M.: *Numerical Heat Transfer,* **8,** 667 (1985).
8. Prata, A.T. and Sparrow, E.M.: *Canad. J. Chem. Eng.*, **64,** 511 (1986).
9. Gosman, A.D., Pun, W.M., Runchal, A.K., Spalding, D.B., and Wolfshtein, M.: Heat and Mass Transfer in Recirculating Flows", Academic Press, London (1973).
10. Chang, H.N., Ryu, H.W., Park, D.H., and Park, Y.S.: *Int'l J. Heat & Mass Transfer,* **30,** 2137 (1987).